

## Neutron Resonances in the keV Region: Odd-Intermediate Nuclei\*

HARVEY MARSHAK† AND HENRY W. NEWSON  
*Department of Physics, Duke University, Durham, North Carolina*  
 (Received December 21, 1956)

The total neutron cross sections of  $\text{Sc}^{45}$ ,  $\text{V}^{51}$ ,  $\text{Mn}^{55}$ ,  $\text{Co}^{59}$ ,  $\text{Cu}^{63}$ , and  $\text{Cu}^{65}$  have been measured in the energy range of  $\sim 1$  to  $\sim 100$  keV. The resonance parameters, including tentative  $J$ -value assignments, have been obtained for some of the more pronounced resonances observed. In the low-energy region, where our measurements overlap with those made with time-of-flight equipment, the results for the 2.36-keV resonance in  $\text{Mn}^{55}$  and the 4.1-keV resonance in  $\text{Sc}^{45}$  are in good agreement.  $\bar{\Gamma}_n^0/\bar{D}$  (averaged between 1 and 100 keV) was determined for Cl, K, Ni<sup>58</sup>, Ni<sup>60</sup>, As<sup>75</sup>, and the above six nuclei. To calculate  $\bar{\Gamma}_n^0/\bar{D}$  the average experimental transmission data was compared to the average Breit-Wigner transmission. The variation of  $\bar{\Gamma}_n^0/\bar{D}$  with atomic weight has been compared to the theoretical predictions of the Feshbach, Porter, and Weisskopf model of the nucleus. The results indicated that the peak is around  $A=47$ , and the amplitude is about  $5 \times 10^{-4}$ . These values would roughly correspond to a real potential,  $V_0=46.5$  Mev, and  $\zeta=0.05$  for the complex fraction of the potential; a square potential well and a radius  $R=1.45A^{1/3} \times 10^{-13}$  were assumed.

### I. INTRODUCTION

STUDIES of total neutron cross sections yield important parameters of nuclear energy levels.<sup>1</sup> The levels observed, are those of the compound nucleus at an excitation energy equal to the neutron binding plus the bombarding energy. The theoretical basis for the resonance phenomena is very well explained by the Breit-Wigner theory.<sup>1-3</sup> In the keV region, the problem is simplified for light and intermediate nuclei since the predominant reaction is elastic scattering. There is a further simplification near  $A=50$ , since we may assume that most of the scattering in this region (1-100 keV) is due to  $s$ -wave neutrons. Although higher angular momentum resonances are present, their half-widths are usually very small due to the centrifugal barrier effect. Thus the resonances observed can be described by the single-level Breit-Wigner scattering formula for  $s$ -wave neutrons. The important parameters which appear in this formula are the energy  $E_0$  of the resonance, its half-width,  $\Gamma$ , and its spin  $J$ . If the resolution distorts the true shape of the resonance, a correction must be applied to the data to obtain the true shape.

An important parameter, which does not appear in the Breit-Wigner formula, is the average level spacing  $\bar{D}$ , which is the average energy separation between two adjoining levels of the same spin and parity. The ratio of the average reduced neutron half-width to the average level spacing for each channel,  $\bar{\Gamma}_n^0/\bar{D}$ , is called the strength function.<sup>4</sup> This function can be compared

with theoretical predictions based on different nuclear models.<sup>3,5</sup>

The region around  $A=50$  is of particular interest in regard to the Feshbach, Porter, and Weisskopf model of the nucleus.<sup>5</sup> Since it is known<sup>6</sup> that the level spacing of the intermediate nuclei are of the order of a few keV, a systematic study of the neutron cross sections of some of these nuclei was undertaken.

### II. APPARATUS AND PROCEDURE

The measurement of total neutron cross sections by the Duke neutron collimation-detection system has been previously described.<sup>7</sup> In some of the latter runs, the energy determination made by measuring the threshold of the  $\text{Li}(p,n)$  reaction has been supplemented by normalizing the energy scale to a low-energy resonance in  $\text{Mn}^{55}$ , reported to be at  $2.36 \pm 0.01$  keV by the Argonne fast chopper group.<sup>8</sup> The method of energy calibration by means of the  $\text{Li}(p,n)$  reaction is somewhat less accurate than that of the fast choppers. The final error in our energy determination is estimated to be  $\pm 1\%$  above 25 keV, and  $\pm 0.25$  keV below 25 keV.

The  $\text{Cu}^{63}$  and  $\text{Cu}^{65}$  samples<sup>9</sup> were in the form of copper oxide powder. The  $\text{Cu}^{63}\text{O}$  and  $\text{Cu}^{65}\text{O}$  samples were 99.40% and 98.16% isotopically pure, respectively. The samples were compressed in the form of a rectangular parallelepiped using a tool steel die and a hydraulic press capable of a ram force of 20 000 pounds. While under pressure, the samples were heated to  $150^\circ\text{C}$  for a few hours to ensure that there was no water vapor in them. They were then hermetically sealed in tight fitting 5-mil silver cases. Silver was used since its cross-section curve is flat at our resolution and energy.<sup>10</sup> The samples were large enough so that

\* This work was supported by the U. S. Atomic Energy Commission.

† Now at Brookhaven National Laboratory, Upton, Long Island, New York.

<sup>1</sup> J. M. Blatt and V. F. Weisskopf, *Theoretical Nuclear Physics* (John Wiley and Sons, Inc., New York, 1952), Chap. VIII.

<sup>2</sup> G. Breit and E. P. Wigner, *Phys. Rev.* **49**, 519 (1936).

<sup>3</sup> Feshbach, Peaslee, and Weisskopf, *Phys. Rev.* **71**, 145 (1947).

<sup>4</sup> Some authors [e.g., R. G. Thomas, *Phys. Rev.* **98**, 77 (1955); S. E. Darden, *Phys. Rev.* **99**, 748 (1955)] prefer to define the strength function by replacing  $\bar{\Gamma}_n^0$  by the Wigner definition of the reduced neutron half-width.

<sup>5</sup> Feshbach, Porter, and Weisskopf, *Phys. Rev.* **96**, 448 (1954).

<sup>6</sup> Hibdon, Langsdorf, and Holland, *Phys. Rev.* **85**, 595 (1952).

<sup>7</sup> J. H. Gibbons, *Phys. Rev.* **102**, 1574 (1956).

<sup>8</sup> Bollinger, Palmer, and Dahlberg, *Phys. Rev.* **95**, 645 (1954).

<sup>9</sup> Enriched isotopes were borrowed from the Isotope Division of the Oak Ridge National Laboratory, Oak Ridge, Tennessee.

<sup>10</sup> Unpublished results from this laboratory.

TABLE I. Results of 57.3-keV resonance in Cu<sup>64</sup>.

$E_0$ (keV)	$J$ value	$\Delta E$ (keV)	$\Gamma_{\text{area}}$ (keV)	Average $\Gamma_{\text{area}}$ (keV) <sup>a</sup>
$57.3 \pm 0.6$	1	3.3	1.32	$1.19 \pm 0.24$
		4.3	1.23	
		5.3	1.03	
	2	3.3	0.76	$0.74 \pm 0.15$
		4.3	0.72	
		5.3	0.73	

<sup>a</sup> The italicized number is the average  $\Gamma_{\text{area}}$  for the preferred  $J$  value of 2.

they intercepted the full area of the neutron beam entering the collimator. To compensate for the effect of the silver jacket and the contaminating isotope, dummy samples were prepared. In the case of the Cu<sup>65</sup>O sample, the dummy sample consisted of 10 mils of silver foil, and the proper thickness of natural copper foil (2 mils), so that it had the same thickness in atoms/cm<sup>2</sup> as the contaminating Cu<sup>63</sup> isotope. Therefore, taking the ratio of the sample-in count of the Cu<sup>65</sup>O sample to its dummy sample, we get the transmission ratio for pure Cu<sup>65</sup>O. Similarly, a dummy sample was prepared for the Cu<sup>63</sup>O sample. For both samples the oxygen cross section can be subtracted out since it is fairly constant at 3.7 barns over the energy region involved.<sup>10,11</sup>

The Co<sup>59</sup>, Mn<sup>55</sup>, and V<sup>51</sup> samples were in the form of metal sheets, ground to the required thickness. The Sc<sub>2</sub><sup>45</sup>O<sub>3</sub>, and As<sup>75</sup> were in the form of fine powders; they were treated in a similar manner to the CuO samples. The estimated error in all the sample thicknesses was less than 1%; and the purities in all cases are 99% or better according to the manufacturers.

For each neutron energy setting, the sample-in and sample-out count were monitored by the integrated proton current striking the lithium target. The neutron counts obtained from a modified McKibben counter placed at 0 degrees to the incident proton beam served as a check on the proton monitoring. The number of counts recorded by the detecting system for the sample-in was usually kept above 5000. The sample-out count was usually taken twice at each energy setting in order to check the consistency of the yield during counting.

The cross-section curves were calculated from the relation  $\sigma_t = (1/N) \ln(1/T)$ , where  $N$  is the sample thickness and  $T$  is the observed transmission ratio. No resolution correction was applied directly to these curves. Since the present resolution is not sufficient to resolve most of the resonances observed, the method of area analysis was used<sup>12</sup> to determine the half-width of a resonance for each of the two possible  $J$  values. This method of analysis does not depend upon knowing the exact shape of the resolution function. The assumptions made are that the resonances are well separated in

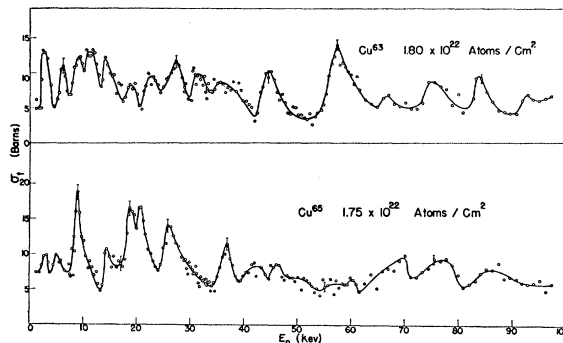


FIG. 1. Total neutron cross sections of Cu<sup>63</sup> and Cu<sup>65</sup> vs energy. Errors indicated are derived from counting statistics.

energy, and that the interference term in the single Breit-Wigner formula can be neglected; that is, on the average, the potential and resonance scattering add incoherently. The estimated total error in  $\Gamma_{\text{area}}$  is about 20%.

By investigating a resonance with two different sample thicknesses, and applying the method of area analysis to both curves, one can in principle determine the  $J$  value of the resonance. The half-width corresponding to the correct  $J$  value should not vary much for different sample thicknesses, whereas the half-widths we calculate, assuming the wrong  $J$  value, will usually vary for different sample thicknesses.

### III. ANALYSIS OF INDIVIDUAL RESONANCES

#### Cu<sup>63</sup>, Cu<sup>65</sup>

The total neutron cross sections of the two copper isotopes were measured from 1.1 to 97.2 keV, Fig. 1. These measurements were made simultaneously, so that comparison with the same resolution could be made. The samples were of about the same thickness. The spins of the ground states of both copper isotopes are  $\frac{3}{2}$ . For  $s$ -wave scattering there are two possible  $J$ -values,  $J=1$ , and  $J=2$ .

The Cu<sup>63</sup> sample showed quite a few resonances in this energy interval, with a particularly strong one at 57.3 keV. The method of area analysis was used to determine  $\Gamma_{\text{area}}$  for the two different  $J$  values. The results for this resonance are given in Table I. The consistency of the  $\Gamma_{\text{area}}$  values calculated for the different energy intervals,  $\Delta E$ , leads to a very slight preference for the  $J=2$  state. Since only one sample thickness was available, the  $J$  value could not be determined uniquely, and the best estimate of  $\Gamma_{\text{area}}$  is taken as the average of the two values given in Table I; that is,  $\Gamma_{\text{area}}$  is roughly 1 keV.

By assuming that all of the resonances observed in the energy region under study are due to  $s$ -wave scattering, and that both spin states occur in equal amounts,<sup>13</sup> a rough estimate of the average level

<sup>11</sup> C. K. Bockelman, Phys. Rev. **80**, 1011 (1950).

<sup>12</sup> E. Merzbacher (private communication).

<sup>13</sup> A recent survey shows that this assumption might not be valid; see V. L. Sailor, Phys. Rev. **104**, 736 (1956).

spacing can be obtained by counting up the number of peaks in an energy interval and dividing by two. Since many of the peaks at higher energy might be double, the first 25 keV was used to determine  $\bar{D}$ . This turns out to be about 7 keV per channel for Cu<sup>64</sup>.

The Cu<sup>65</sup> sample showed somewhat less structure than the Cu<sup>63</sup> sample. For Cu<sup>66</sup> the average level spacing per channel is about 8.5 keV.

### V<sup>51</sup>, Mn<sup>55</sup>, Co<sup>59</sup>

The total neutron cross sections of V<sup>51</sup>, Mn<sup>55</sup>, and Co<sup>59</sup> were measured from 1.6 to 100.5 keV, Fig. 2. These measurements were made simultaneously, so that comparison with the same resolution could be made. The samples were of about the same thickness. The energy scale was normalized so that the resonance apparently at 2.6 keV in Mn<sup>56</sup> was shifted to 2.36 keV<sup>8</sup> as mentioned previously.

One can get some idea as to where the resolution of current time-of-flight equipment begins to exceed the resolution of our equipment by comparing some low-energy resonances. The 2.36-keV resonance in Mn<sup>56</sup> is resolved by a fast chopper and a peak cross section of 650 barns is measured,<sup>8</sup> which agrees with the theoretical value for  $J=3$ . The peak cross section of this resonance is 150 barns when measured under the

best prevailing resolution and background conditions of our equipment. The 7.3- and 9.0-keV resonances in Mn<sup>56</sup> appear as one peak when investigated with the Argonne<sup>8</sup> and Brookhaven<sup>14</sup> fast choppers. Thus it seems that, above 5 keV, our equipment has better resolution than the current time-of-flight devices with which we can make this comparison.<sup>14</sup>

The spins of the ground state of V<sup>51</sup>, Mn<sup>55</sup>, and Co<sup>59</sup> are  $\frac{7}{2}$ ,  $\frac{5}{2}$ , and  $\frac{7}{2}$ , respectively. Assuming  $s$ -wave scattering, the  $J$  values for V<sup>51</sup> and Co<sup>59</sup> are  $J=3$  and  $J=4$ , while for Mn<sup>55</sup> the  $J$  values are  $J=2$  and  $J=3$ . In Fig. 2 the loci of points for the peak cross sections have been drawn in for the pertinent  $J$  values. In looking at the three cross-section curves, one notices that they all have about the same number of resonances. The average level spacing for V<sup>52</sup>, Mn<sup>56</sup>, and Co<sup>60</sup> are 10, 10, and 8.5 keV respectively, for the first 25 keV. The size of the resonances (observable half-widths) decrease as we go from V<sup>52</sup> to Mn<sup>56</sup> to Co<sup>60</sup>. Thus, one can qualitatively see that the strength function is largest for vanadium and decreases as we go to manganese and cobalt.

The circles in Fig. 2 represent the cross section taken with a sample of one-half the thickness of that used to take the solid cross-section curves. Most of the peaks are noticeably higher for the thinner samples because of self-shielding and background. Three resonances, two in V<sup>52</sup> at 69.1 and 87.1 keV, and one in Mn<sup>56</sup> at 35.1 keV appear to be nearly perfectly resolved; that is, the circles at the peaks fall very near the dashed lines. These three resonances were looked at with thinner samples and better statistics; the results of these later measurements are given in Table II. The directly measured half-widths,  $\Gamma_{\text{exp}}$ , are in good agreement with the  $\Gamma_{\text{area}}$ , calculated by the area analysis for the two vanadium resonances; the manganese peak at 35.1 keV may be complex, in which case neither method of analysis is applicable.

The peaks of the first three resonances at 4.1, 6.6, and 11.5 keV in V<sup>52</sup>, were re-examined very carefully with samples as thin as  $0.192 \times 10^{22}$  atoms/cm<sup>2</sup>. Although the measured maximum cross sections were high, they did not come up to either of the two  $J$ -value curves, and were not perfectly resolved. By using two different

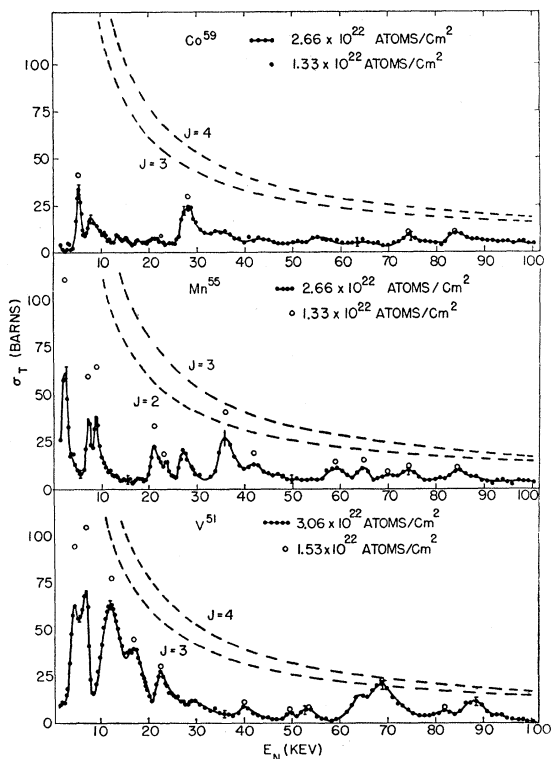


FIG. 2. Total neutron cross sections of V<sup>51</sup>, Mn<sup>55</sup> and Co<sup>59</sup> vs energy. Assuming  $s$ -wave scattering, the theoretical maximum cross sections are drawn in for the two different  $J$  values.

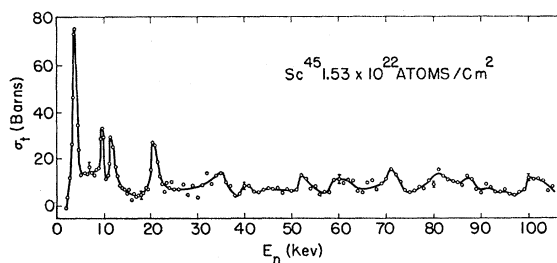


FIG. 3. Total neutron cross section of Sc<sup>45</sup> vs energy.

<sup>14</sup> Seidl, Hughes, Palevsky, Levin, Kato, and Sjöstrand, Phys. Rev. 95, 476 (1954).

TABLE II. Summary of neutron half-widths and  $J$ -value assignments.  $E_0$  is the neutron energy at the peak of the resonance.  $\Gamma_{\text{area}}$  is the neutron half-width computed by the area analysis method.  $\Gamma_{\text{exp}}$  is the measured half-width of the resonance.  $\sigma_{\text{so}}$  is the maximum theoretical cross section obtained by using the single-level Breit-Wigner formula.  $\sigma_{\text{exp}}$  is the experimentally measured peak cross section.

Target nucleus	$E_0$ (keV)	$\Gamma_{\text{area}}$ (keV) <sup>a</sup>		$\Gamma_{\text{exp}}$ (keV)	$\sigma_{\text{so}}$ (barns)		$\sigma_{\text{exp}}$ (barns)	Preferred $J$ value
		$J = I + \frac{1}{2}$	$J = I - \frac{1}{2}$		$J = I + \frac{1}{2}$	$J = I - \frac{1}{2}$		
Sc <sup>45</sup>	4.1 ± 0.25 <sup>b</sup>	0.22 ± 0.04	0.26 ± 0.05	...	365	283	116 ± 5	...
V <sup>51</sup>	4.1 ± 0.25 <sup>b</sup>	0.41 ± 0.08	0.48 ± 0.10	...	365	283	158 ± 6	4
		0.44 ± 0.09	0.53 ± 0.11					
Mn <sup>55</sup>	6.6 ± 0.25 <sup>b</sup>	0.48 ± 0.10	0.56 ± 0.11	...	230	178	104 ± 4	4
		0.51 ± 0.10	0.62 ± 0.12					
	11.5 ± 0.25 <sup>b</sup>	2.26 ± 0.45	2.85 ± 0.57	...	133	104	81 ± 3	4
		2.26 ± 0.45	3.12 ± 0.62					
	16.6 ± 0.25	1.9 ± 0.38	2.4 ± 0.48	...	93	74	39 ± 1.5	...
	22.1 ± 0.25	1.0 ± 0.20	1.3 ± 0.26	...	69	56	26 ± 1.0	...
	69.1 ± 0.7 <sup>c</sup>	4.5 ± 0.90	6.0 ± 1.2	5.0	24	20	26 ± 1.0	4
	87.1 ± 0.9 <sup>c</sup>	2.2 ± 0.44	2.8 ± 0.56	3.0	20	17	15 ± 0.5	3
	2.36 ± 0.25 <sup>b</sup>	0.31 ± 0.06	0.37 ± 0.07	...	658	470	150 ± 6	3
		0.35 ± 0.07	0.43 ± 0.09					
Co <sup>60</sup>	7.3 ± 0.25 <sup>b</sup>	0.23 ± 0.05	0.28 ± 0.06	...	212	151	73 ± 3	...
	9.0 ± 0.25 <sup>b</sup>	0.64 ± 0.13	0.78 ± 0.16	...	172	123	73 ± 3	...
	21.2 ± 0.25	0.42 ± 0.08	0.55 ± 0.11	...	73	52	24 ± 1	...
	27.3 ± 0.3	0.89 ± 0.18	1.2 ± 0.24	...	57	41	20 ± 1	...
	35.1 ± 0.4 <sup>c</sup>	1.4 ± 0.28	2.0 ± 0.40	2.8	46	33	43 ± 1.5	3
	4.7 ± 0.25 <sup>b</sup>	0.32 ± 0.06	0.37 ± 0.07	...	322	250	120 ± 5	...
	7.8 ± 0.25	0.22 ± 0.04	0.26 ± 0.05	...	192	149	18 ± 0.5	...
	28.3 ± 0.3	1.1 ± 0.22	1.5 ± 0.30	...	56	45	24 ± 1	...

<sup>a</sup> The italicized numbers indicate the value of  $\Gamma_{\text{area}}$  for the preferred  $J$  values.

<sup>b</sup> These resonances were analyzed by using two different sample thicknesses. In the case where a preferred  $J$  value is given, both values of  $\Gamma_{\text{area}}$  are also given.

<sup>c</sup> These resonances were considered to be perfectly resolved.

sample thicknesses, the first three resonances in V<sup>52</sup>, along with the 2.36-, 7.3-, and 9.0-keV resonances in Mn<sup>56</sup>, and the 4.7-keV resonance in Co<sup>60</sup> were investigated. The results for these resonances are given in Table II. The experimental peak cross sections are for the thinner samples.

The  $J$ -value assignment for the 2.36-keV resonance in Mn<sup>56</sup> agrees with the results of the Argonne group.<sup>8</sup> They report a half-width of  $0.34 \pm 0.03$  keV, whereas here the average for the two samples for the  $J=3$  state is  $0.33 \pm 0.07$  keV.

By using the data of Fig. 2, some of the remaining larger resonances were also analyzed by the method of area analysis. These results are given in Table II.

### Sc<sup>45</sup>

The total neutron cross section of Sc<sup>45</sup> was measured from 2.0 to 105.0 keV, Fig. 3. The average level spacing per channel for the first 25 keV is about 12 keV. The sizes of the resonances (observable half-widths) are about the same size as those in Mn<sup>56</sup>. Thus, we can qualitatively see that the strength function has a maximum in the neighborhood of vanadium.

The 4.1-keV resonance in Sc<sup>45</sup> was reinvestigated with two sample thicknesses at the same time as the other low-energy resonances discussed in the last section. The results are given in Table II. This resonance was also investigated by the Harwell fast chopper group.<sup>15</sup> They report it at  $3.6 \pm 0.2$  keV, with a half-

width of approximately 0.18 keV as compared to our value of  $0.22 \pm 0.04$  keV for the upper  $J$  value.

## IV. DISCUSSION OF RESULTS

A good many assumptions are implied in the application of the area method, and in general the resulting estimates of the half-widths are not very accurate. In Table II, variation of  $\Gamma_{\text{area}}$  with the choice of  $J$  value is not much greater than the experimental error from other causes; hence, when no preference is indicated by the data, a useful estimate of the half-width may be made by averaging the values for the two different  $J$  values. Conversely, a strong preference for one  $J$  value will appear only under very favorable circumstances; the preferences indicated are tentative.

The average level spacing, as obtained by counting the resonant peaks, is subject to considerable uncertainty. It is now known<sup>16,17</sup> that the resonances due to a single channel vary in width over such wide ranges that, in these experiments, some of the resonances are too narrow to detect. In the next section, it is shown clearly that the average strength of the resonances decreases steadily between vanadium and copper. Thus, the correction for lost resonances are larger for copper than for the rest. Time-of-flight work<sup>18</sup> indicates that the spacing per channel for copper may

<sup>16</sup> Harvey, Hughes, Carter, and Pilcher, Phys. Rev. **99**, 10 (1955).

<sup>17</sup> D. J. Hughes and J. A. Harvey, Phys. Rev. **99**, 1032 (1955).

<sup>18</sup> Bollinger, Cote, and LeBlanc (unpublished).

<sup>15</sup> N. J. Pattenden, Proc. Phys. Soc. (London) **A68**, 104 (1955).

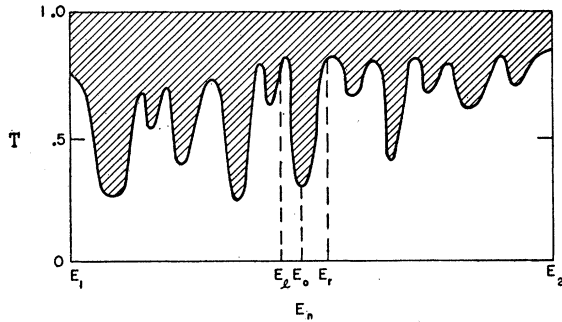


FIG. 4. Example of a transmission curve showing resonance structure.

be as low as 1 or 2 kev for each isotope as compared to the 7-8.5 kev found here.

### V. $\bar{\Gamma}_n^0/\bar{D}$

#### A. Method of Calculation

The ratio of the average reduced neutron width to the average level spacing,  $\bar{\Gamma}_n^0/\bar{D}$ , can be determined experimentally in a number of ways. The straightforward method, which is impracticable in our case, would be to locate all the resonances in a given channel and determine the half-widths. A second method of determining the strength function has been suggested by Thomas,<sup>19</sup> and used by Darden.<sup>20</sup> This method was not used, since one would have to use very thick samples. We considered that the resulting low transmission ratios could not be corrected for background with sufficient accuracy. The method used to calculate  $\bar{\Gamma}_n^0/\bar{D}$  was to compare the average experimental transmission data with the average Breit-Wigner transmission.

The expression relating  $\bar{\Gamma}_n^0/\bar{D}$  to the average experimental transmission can be derived in the following manner. Consider an *s*-wave resonance at energy  $E_0$ , between the energy limits  $E_l$  and  $E_r$ , Fig. 4. The area above the transmission curve is

$$\int_{E_l}^{E_r} (1-T)dE = \int_{E_l}^{E_r} (1 - e^{-N\sigma_{sc}})dE \quad (V-1)$$

where  $T$  is the transmission ratio,  $N$  is the sample thickness, and  $\sigma_{sc}$  is the Breit-Wigner single level scattering formula. Putting this formula into the above equation and evaluating some integrals we obtain the approximate expression

$$\int_{E_l}^{E_r} (1-T)dE = \frac{\alpha}{2} \Gamma_n^0 f(g) + (1-\alpha)(E_l - E_r), \quad (V-2)$$

with

$$\begin{aligned} \alpha &= e^{-N\sigma_{pot}}, \\ f(g) &= (E_0/\epsilon_0)^{1/2} \pi \gamma e^{-1/2} [J_0(\frac{1}{2}i\gamma) - iJ_1(\frac{1}{2}i\gamma)] (1 - \gamma^2 \gamma), \\ \gamma &= 4\pi \lambda_0^2 g N \cos(2kR), \\ \gamma &= \frac{1}{2} \tan(2kR), \end{aligned}$$

where  $\Gamma_n^0$  is the reduced neutron half-width,  $\sigma_{pot}$  is the potential scattering,  $\epsilon_0$  is 1 ev,  $\lambda_0$  is  $(1/2\pi)$  times the neutron de Broglie wavelength at resonance,  $k$  is the neutron wave number,  $R$  is the nuclear radius, and  $g$  is the statistical weight factor.

If we have an energy interval between  $E_1$  and  $E_2$ , composed of numerous resonances of either channel, then we can sum (V-2) approximately to give

$$\int_{E_1}^{E_2} (1-T)dE = \frac{\alpha}{2} \left[ \sum_{n_1} \Gamma_{n_1}^0 f(g_1) + \sum_{n_2} \Gamma_{n_2}^0 f(g_2) \right] + (1-\alpha)(E_2 - E_1), \quad (V-3)$$

where the summations are over the  $n_1$  resonances of channel 1, and the  $n_2$  resonances of channel 2. It has been assumed that the resonances are non-overlapping, and that the potential scattering is constant over the entire energy interval. In practice when the spin is  $> \frac{1}{2}$ ,  $f(g_1)$  is very close in value to  $f(g_2)$ , and one may write

$$\begin{aligned} (1-T)_w &= \int_{E_1}^{E_2} (1-T)dE / \int_{E_1}^{E_2} dE \\ &= \frac{\alpha}{2(E_2 - E_1)} n \bar{\Gamma}_n^0 f(g) + (1-\alpha), \quad (V-4) \end{aligned}$$

where

$$n \bar{\Gamma}_n^0 = \sum_{n_1} \Gamma_{n_1}^0 + \sum_{n_2} \Gamma_{n_2}^0.$$

The average level spacing,  $\bar{D}$ , in the energy interval  $E_1$  to  $E_2$  is defined as

$$\bar{D} = (E_2 - E_1) / \frac{1}{2} n, \quad (V-5)$$

TABLE III. Summary of the values of  $(\bar{\Gamma}_n^0/\bar{D})_1$  calculated from the experimental data.<sup>a</sup>

Target nucleus	$10^4 \times (\bar{\Gamma}_n^0/\bar{D})_1$	$10^4 \times$ Estimated error	Sample thickness ( $10^{22}$ atoms/cm <sup>2</sup> )
C <sup>135</sup>	0.0059	$\pm 0.3$	5.69
K <sup>39</sup>	-0.78	$\pm 0.3$	6.23
Sc <sup>45</sup>	3.5	$\pm 0.9$	1.53
V <sup>51</sup>	4.7	$\pm 0.4$	3.06
Mn <sup>55</sup>	3.3	$\pm 0.5$	2.66
Ni <sup>58</sup>	3.4	$\pm 1.0$	3.13
Co <sup>59</sup>	1.9	$\pm 0.6$	2.66
Ni <sup>60</sup>	2.3	$\pm 1.0$	3.06
Cu <sup>63</sup>	1.6	$\pm 0.8$	1.80
Cu <sup>65</sup>	2.0	$\pm 0.8$	1.75
As <sup>75</sup>	3.6	$\pm 0.5$	3.06

<sup>19</sup> R. G. Thomas, Phys. Rev. 98, 77 (1955).

<sup>20</sup> S. E. Darden, Phys. Rev. 99, 748 (1955).

<sup>a</sup>  $(\bar{\Gamma}_n^0/\bar{D})_1$  was calculated by using Eqs. (V-6) and (V-7), with  $\sigma_{pot} = 4\pi R^2$ .

where we assumed  $n_1 = n_2 = \frac{1}{2}n$ . Combining Eqs. (V-4) and (V-5), we obtain

$$\frac{\bar{\Gamma}_n^0}{\bar{D}} = \frac{1}{\alpha} \left[ \frac{\langle 1-T \rangle_{Av} - (1-\alpha)}{f(g)} \right]. \quad (V-6)$$

For nuclei with  $I=0$  (even  $A$ , with the exception of the odd-odd nuclei), there is only one  $g$  value for  $s$ -wave neutrons; one has instead

$$\frac{\bar{\Gamma}_n^0}{\bar{D}} = \frac{2}{\alpha} \left[ \frac{\langle 1-T \rangle_{Av} - (1-\alpha)}{f(g)} \right]. \quad (V-7)$$

The parameter  $\alpha$ , which is determined by the potential scattering, can be evaluated either from the cross-section data or on the basis of some nuclei model; e.g., for the strongly absorbing or "black nucleus" model<sup>3</sup>  $\sigma_{pot} = 4\pi\lambda^2 \sin^2 kR$ .

Since  $\bar{D}$  presumably does not vary much from subinterval to subinterval, we can define  $\bar{\Gamma}_n^0/\bar{D}$  for the entire energy range:

$$\frac{\bar{\Gamma}_n^0}{\bar{D}} = \frac{\sum_i (\bar{\Gamma}_n^0/\bar{D})_i \Delta E_i}{\sum_i \Delta E_i}. \quad (V-8)$$

### B. Comparison with Theory

The equations derived in the last section can now be used to determine the strength function. The potential scattering cannot be obtained from inspection of the cross-section curves because of the large widths of the resonances and the very wide interference terms. In order to evaluate the strength function, theoretical values for  $\sigma_{pot}$  must be used in addition to the experimental values of  $\langle 1-T \rangle_{Av}$ . As a first approximation, it will be assumed that  $\sigma_{pot} = 4\pi R^2$ , and  $R = 1.45 \times 10^{-13} A^{\frac{1}{3}}$  cm. These assumptions correspond to the "black nucleus" model. The values so obtained will be designated by  $(\bar{\Gamma}_n^0/\bar{D})_1$ . The transmission data used to calculate the strength function was taken over approximately the same energy region for all of the samples ( $\sim 1$  to  $\sim 100$  kev). Using the transmission data from Figs. 1, 2, and 3, the strength function was determined for  $\text{Cu}^{65}$ ,  $\text{Cu}^{63}$ ,  $\text{Co}^{59}$ ,  $\text{Mn}^{55}$ ,  $\text{V}^{51}$ , and  $\text{Sc}^{45}$ . The transmission curves for natural chlorine and

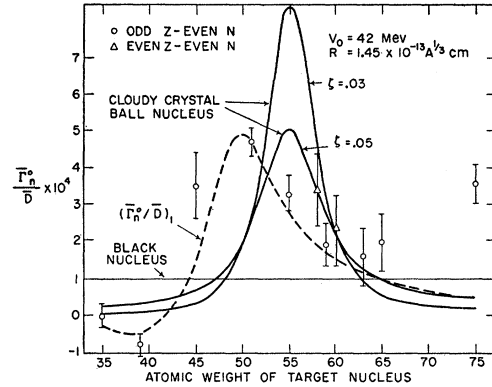


FIG. 5. The experimental values of  $(\bar{\Gamma}_n^0/\bar{D})_1$  are compared to the theoretical predictions of the "black" and "cloudy crystal ball" models of the nucleus.  $(\bar{\Gamma}_n^0/\bar{D})_1$  is only a first approximation to  $\bar{\Gamma}_n^0/\bar{D}$ , since it assumes that the potential scattering is constant, namely  $4\pi R^2$ . The dashed curve is the calculated value of  $(\bar{\Gamma}_n^0/\bar{D})_1$  for the parameters  $V_0 = 46.5$  Mev,  $\zeta = 0.5$ , which gives the best fit to the experiment data.

natural potassium taken respectively by Patterson<sup>21</sup> and Toller<sup>22</sup> at this laboratory were used to calculate the strength function. Natural chlorine is 75.4%  $\text{Cl}^{35}$ , and 24.6%  $\text{Cl}^{37}$ , while natural potassium is 93.1%  $\text{K}^{39}$ , and 6.9%  $\text{K}^{41}$ . In both cases the calculation was made assuming both samples were composed entirely of the major isotope. The two nickel isotopes,  $\text{Ni}^{58}$  and  $\text{Ni}^{60}$ , used to obtain the transmission data for the calculation of the strength function by Block<sup>23</sup> at this laboratory, were practically isotopically pure. The results of all these calculations are given in Table III.

Since all the samples used were not of the same thickness (see Table III), an experiment was performed to check this effect on the calculation of  $(\bar{\Gamma}_n^0/\bar{D})_1$ ; five different nuclei,  $\text{Sc}^{45}$ ,  $\text{V}^{51}$ ,  $\text{Mn}^{55}$ ,  $\text{Co}^{59}$ , and  $\text{As}^{75}$ , were prepared in two sample thicknesses. The thin sample was  $0.765 \times 10^{22}$  atoms/cm<sup>2</sup>, and the other one was four times as thick. The results are given in Table IV. From this experiment, it was concluded that the assumptions used to calculate  $(\bar{\Gamma}_n^0/\bar{D})_1$  are reasonably accurate for a considerable range of sample thicknesses. The measurement of the thicker  $\text{Sc}^{45}$  sample in this second experiment was spoiled by misalignment.

The errors quoted in Table III were computed by assuming that a 2% point-by-point error in the transmission data was not improved by averaging over many points. The statistical error is much overestimated, but the errors estimated by the reproducibility of the data in Table IV are about this order of magnitude.

In Fig. 5, the data from Table III are plotted as a function of the atomic weight ( $A$ ) of the target nucleus. The calculated values of  $(\bar{\Gamma}_n^0/\bar{D})_1$  are compared to the

TABLE IV.  $(\bar{\Gamma}_n^0/\bar{D})_1$  determined from the experimental data of a thick and thin sample.

Target nucleus	Thin sample <sup>a</sup>	$10^4 \times (\bar{\Gamma}_n^0/\bar{D})_1$ Thick sample <sup>b</sup>	Results from Table III
$\text{Sc}^{45}$	4.0	0.17	3.5
$\text{V}^{51}$	4.7	4.4	4.7
$\text{Mn}^{55}$	3.7	2.5	3.3
$\text{Co}^{59}$	2.6	2.2	1.9
$\text{As}^{75}$	3.9	3.6	...

<sup>a</sup> The thin sample was  $0.765 \times 10^{22}$  atoms/cm<sup>2</sup>.

<sup>b</sup> The thick sample was  $3.06 \times 10^{22}$  atoms/cm<sup>2</sup>.

<sup>21</sup> R. P. Patterson, Ph. D. thesis, Duke University, 1954 (unpublished).

<sup>22</sup> A. L. Toller, Ph. D. thesis, Duke University, 1954 (unpublished).

<sup>23</sup> R. C. Block, Ph. D. thesis, Duke University, 1955 (unpublished).

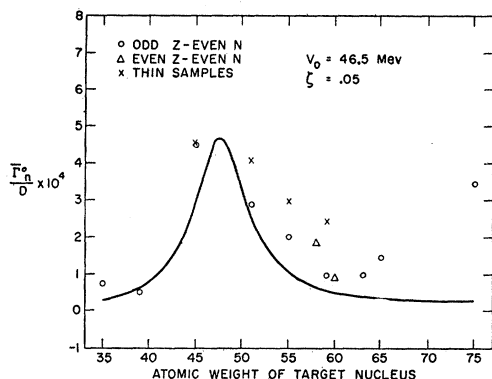


FIG. 6. The values of  $\bar{\Gamma}_n^0/\bar{D}$  are compared to the theoretical predictions of the "cloudy crystal ball" model of the nucleus.

theoretical predictions of the "black nucleus" model for  $V_0=42$  Mev (horizontal line). These values can also be used as a first approximation to  $\bar{\Gamma}_n^0/\bar{D}$  as predicted by the "cloudy crystal ball" model of Feshbach, Porter, and Weisskopf. The "cloudy crystal ball" prediction is plotted for the parameters  $V_0=42$  Mev,  $\zeta=0.03$ , and  $\zeta=0.05$  (solid curves). It is obvious that  $\zeta=0.05$  gives the better agreement, and that a considerable higher value of  $V_0$  is indicated. A method of successive approximations must be used to obtain a more accurate comparison with this theory, since the value of  $R'$  used in determining the potential scattering changes with each choice of the parameters. As a second approximation, theoretical values of  $(\bar{\Gamma}_n^0/\bar{D})_{1\frac{1}{2}}$  may be calculated from the "cloudy crystal ball" model by subtracting the effect of the difference due to  $(R^2-R'^2)$  from the theoretical values of  $\bar{\Gamma}_n^0/\bar{D}$ . The parameters were adjusted to fit the experimental data:  $V_0=46.5$  Mev,  $\zeta=0.05$  (dashed curve). It is interesting to note that the experimental values for  $(\bar{\Gamma}_n^0/\bar{D})_1$  show the asymmetry to be expected from theory. The negative value for potassium indicates that the average total cross section is less than  $4\pi R^2$ , the "black nucleus" value for the potential scattering alone. Figure 6 shows the theoretical curve of the strength function,  $\bar{\Gamma}_n^0/\bar{D}$ , and the points calculated from the experimental data and the parameters determined in Fig. 5 (dashed curve). For comparison, values for the strength function calculated from thin-sample transmission measurements (Table IV) are also shown in Fig. 6 (crosses), for the cases where the data are available. This is an indication

‡ *Note added in proof.*—The dashed curve in Fig. 5 was calculated essentially by means of the equation  $(\bar{\Gamma}_n^0/\bar{D})_1 = (\bar{\Gamma}_n^0/\bar{D}) [1 - 4\pi N(R^2 - R'^2)] - 4\pi N(R^2 - R'^2) \langle f(g^{-1}) \rangle_{AV}$ , where  $\langle f(g^{-1}) \rangle_{AV}$  is obtained by averaging over the energy range of the cross-section curves. A point was calculated for each experimental point in Fig. 5 using the sample thickness of that measurement and theoretical values for  $R'$  and the strength function calculated from the square well complex potential model with the parameters indicated. These theoretical points were connected by the dashed curve in the figure.

that the errors due to the use of rather large sample thicknesses are of the order of the errors in Fig. 5. It would have improved the accuracy in the calculation of the strength function if all the transmission measurements were made with thin samples.‡

It should be noted that, while  $(\bar{\Gamma}_n^0/\bar{D})_1$  is calculated from the experimental data in a straightforward manner, a particular model, and associated parameters had to be assumed before the quantity  $\bar{\Gamma}_n^0/\bar{D}$  could be evaluated. Theoretical calculations based on any other model should be compared to the points in Fig. 5 rather than those in Fig. 6. More elaborate theories using a more realistic well shape<sup>24,25</sup> would no doubt lead to somewhat different parameters for the same experimental data.

The As<sup>75</sup> point is very much higher than the curve in Fig. 6; however the details of the spectrum at low energies are well known<sup>18</sup> and the value for the potential scattering is about 8.5 barns. If the experimental value of 8.5 barns is used instead of the theoretical value of  $4\pi R'^2 \approx 5$  barns, the As<sup>75</sup> point falls very close to the theoretical curve.

The Argonne fast chopper group has also measured the strength function in the region around  $A=50$ .<sup>26</sup> They find that the peak is approximately at  $V^{51}$ , with a much higher amplitude ( $\bar{\Gamma}_n^0/\bar{D} \approx 13 \pm 5 \times 10^{-4}$ ) than ours.<sup>27</sup> The Argonne group measured the half-widths and level spacing of individual resonances to determine the strength function. When comparing our measurements to those of the Argonne group it must be remembered that they analyzed resonances only up to 10–20 kev. If one uses only the first 25 kev of our transmission data to calculate the strength function, the position of the peak is at  $V^{51}$  with an amplitude of approximately  $10 \times 10^{-4}$ . Although the Argonne results are in reasonably good agreement with ours, it seems most likely that the region from  $\sim 1$  to  $\sim 25$  kev includes too few resonances (only 5 visible in  $V^{51}$ ) to be a good statistical sample of the spectrum.

#### ACKNOWLEDGMENTS

It is a pleasure to acknowledge the help of Dr. E. Merzbacher, Dr. W. Haerberli, Dr. R. C. Block, Dr. M. M. Duncan, Dr. J. H. Gibbons, Dr. R. M. Williamson, A. K. Furr, A. Taylor, and other members of the Van de Graaff group at various phases of this investigation.

§ *Note added in proof.*—The poor agreement between the thin sample points in Fig. 6 and the theoretical curve is probably due either to departure from a square well potential or from the arbitrarily chosen and rather high value,  $R=1.45 A^{1/3} \times 10^{-13}$ , or both.

<sup>24</sup> R. D. Woods and D. S. Saxon, Phys. Rev. **95**, 577 (1954).

<sup>25</sup> Morrison, Muirhead, and Murdoch, Phil. Mag. **46**, 795 (1955).

<sup>26</sup> R. Cote and L. M. Bollinger, Phys. Rev. **98**, 1162(A) (1955).

<sup>27</sup> A curve of the Argonne results can be found in a paper by V. F. Weisskopf, *Proceedings of the International Conference on the Peaceful Uses of Atomic Energy, Geneva, 1955* (United Nations, New York, 1956), Vol. 2, p. 27.